Bit Error Probability of Space Modulation over Nakagami-m Fading: Asymptotic Analysis

Marco Di Renzo, Harald Haas

Bit Error Probability of Space Modulation over Nakagami–m Fading – Asymptotic Analysis

Marco Di Renzo *Member, IEEE*, and Harald Haas, *Member, IEEE*

***Abstract*— Recently, the Average Bit Error Probability (ABEP) of Space Shift Keying (SSK) and Spatial Modulation (SM) over Nakagami–*m* fading has been computed as a single integral involving the Meijer–G function. Even though the frameworks are very accurate, the use of special functions hides some fundamental properties of the aforementioned new modulation schemes, *e.g.*, coding and diversity gains. In this Letter, we exploit a notable limit involving the Meijer–G function near the singular point -1, and provide a simple, closed–form, and asymptotically tight upper–bound of the ABEP. The result is applicable to SM and SSK modulation, to correlated Nakagami–*m* fading, and to general Multiple–Input Multiple–Output (MIMO) wireless systems. As a case study, numerical examples showing the accuracy for SSK modulation are given, and it is proved that, unlike conventional modulations, the diversity gain is independent of the fading severity *m*.**

***Index Terms*— Spatial modulation, space shift keying modulation, Nakagami–*m* fading, Meijer–G function, asymptotic analysis, diversity gain, coding gain.**

I. Introduction

SPACE modulation is a digital modulation concept for Multiple–Input Multiple–Output (MIMO) wireless systems [1]–[3]. Recent results have shown that it can outperform many state–of–the–art transmission technologies [1]–[9]. The fundamental innovation is the introduction of the so–called spatial constellation diagram, which is used for data modulation. More specifically, improved performance is not achieved through the simultaneous transmission of multiple data streams, but by encoding the information bits onto the spatial positions of the antennas at the transmitter [3].

Two basic space modulation concepts exist in the literature. 1) Space Shift Keying (SSK) modulation [4], where the incoming bitstream is used to identify a single antenna of the antenna–array that is switched on for transmission. The information bits are mapped onto the channel impulse responses of the end–to–end wireless links. The main benefit of SSK modulation is a low implementation complexity. 2) Spatial Modulation (SM) [3], which is a hybrid modulation scheme combining Phase Shift Keying (PSK) or Quadrature Amplitude Modulation (QAM) with SSK modulation. In SM, each block of information bits is transmitted through two information–carrying units: some bits are modulated using either PSK or QAM, while the others using SSK modulation. The main benefit of SM is a multiplexing gain, which is obtained with only a single active antenna.

Recently, the Average Bit Error Probability (ABEP) of space modulation over fading channels has been extensively studied [4], [10]–[13]. In particular, special attention has been given to compute the ABEP over Nakagami–m fading, because of the generality of this distribution and its excellent agreement with measurements. To date, very accurate frameworks have been proposed for arbitrary correlated Nakagami–m fading and MIMO setups, which are useful for SSK modulation [11] and SM [10]. In spite of being very accurate, these frameworks need the computation of a single integral involving the Meijer–G function [14], which hides important properties of the system, such as the diversity and coding gains. For example, numerical results in [11] have shown that, unlike PSK/QAM [15], the diversity gain of SSK modulation is independent of the fading severity m. However, this finding cannot be captured through direct inspection of the Meijer–G function.

To have a deeper understanding of the performance of space modulation, in this Letter we propose a simple yet asymptotically tight upper–bound of the ABEP over Nakagami–m fading, which is insightful enough to show diversity and coding gains. The framework is in closed–form, is applicable to SM and SSK modulation, and avoids special functions.

This Letter is organized as follows. In Section II and Section III, the problem is introduced and the main result is given, respectively. In Section IV, diversity and coding gains of SSK modulation are studied. In Section V, some numerical examples are shown. Finally, Section VI concludes this Letter.

II. Problem Statement

From [10] and [11], it follows that the computation of the ABEP of SM and SSK modulation requires the solution of:

$$I = \frac{1}{\pi}\int_0^{\pi/2}\left[\prod_{l=1}^{L}\mathcal{F}_l\left(\frac{\mathrm{SNR}}{2\sin^2(\theta)}\right)\right]d\theta \qquad (1)$$

where SNR denotes the Signal–to–Noise–Ratio (SNR), and $\mathcal{F}_l(\cdot)$ is defined as ($l = 1, 2, \ldots, L$):

$$\begin{aligned}\mathcal{F}_l(s) = {} & \mathcal{K}_l\left(s+\mathcal{X}_{1,l}\right)^{-\omega_{1,l}}\left(s+\mathcal{X}_{2,l}\right)^{-\omega_{2,l}} \\ & \times G_{2,2}^{1,2}\left(-\frac{s^2}{\left(s+\mathcal{X}_{1,l}\right)\left(s+\mathcal{X}_{2,l}\right)}\left|\begin{matrix}1-\omega_{2,l} & 1-\omega_{1,l}\\ 0 & 0\end{matrix}\right.\right)\end{aligned} \qquad (2)$$

and: i) $\mathcal{X}_{1,l}$, $\mathcal{X}_{1,l}$, and $\mathcal{K}_l$ are positive real numbers; ii) $\omega_{1,l}$ and $\omega_{2,l}$ are real numbers; iii) s is a complex number; and iv) $G_{p,q}^{m,n}\left(\cdot\left|\begin{matrix}(a_p)\\(b_q)\end{matrix}\right.\right)$ is the Meijer–G function defined in [14].

In [10] and [11], no closed–form solution of the integral in (1) is given, and numerical integration is used. Although the computational complexity is low and the final result is very accurate, the major limitation of (1) is the difficulty of estimating diversity and coding gains [16], which are useful performance metrics to understand the role of fading severity.

Manuscript received April 24, 2011; revised July 14, 2011; accepted July 26, 2011. The associate editor coordinating the review of this letter and approving it for publication was Diomidis Michalopoulos.

M. Di Renzo is with the Laboratory of Signals and Systems (L2S), CNRS–SUPELEC–Univ. Paris–Sud 11, Paris, France (e–mail: marco.direnzo@lss.supelec.fr).

H. Haas is with the Institute for Digital Communications (IDCOM), The University of Edinburgh, Edinburgh, UK (e–mail: h.haas@ed.ac.uk).

Digital Object Identifier XXX.

III. Main Result

To avoid the limitations in Section II, *Proposition 1* provides a closed–form solution of (1) for high SNR, *i.e.*, $\mathrm{SNR} \gg 1$.

Proposition 1: The integral in (1) can be computed as:

$$I \overset{\mathrm{SNR}\gg 1}{=} \frac{2^{L-1}\left[\prod_{l=1}^{L} b_l\right]\Gamma\left(L+1/2\right)}{\sqrt{\pi}\Gamma\left(L+1\right)}\mathrm{SNR}^{-L} \tag{3}$$

where $\Gamma\left(z\right) = \int_0^{+\infty} x^{z-1}\exp\left(-x\right)dx$, and:

$$b_l = \mathcal{K}_l\left(\mathcal{X}_{1,l}+\mathcal{X}_{2,l}\right)^{-\left(\omega_{1,l}+\omega_{2,l}-1\right)}\Gamma\left(\omega_{1,l}+\omega_{2,l}-1\right) \tag{4}$$

Proof: I in (3) can be obtained by using [16, Prop. 3] with:

$$\lim_{|s|\to\infty}\left[\prod_{l=1}^{L}\left|\mathcal{F}_l\left(s\right)\right|\right] = b\left|s\right|^{-d} + o\left(\left|s\right|^{-d}\right) \tag{5}$$

where $b = \prod_{l=1}^{L} b_l$, $d = \sum_{l=1}^{L} d_l$, and:

$$\lim_{|s|\to\infty}\left|\mathcal{F}_l\left(s\right)\right| = b_l\left|s\right|^{-d_l} + o\left(\left|s\right|^{-d_l}\right) \tag{6}$$

The parameters b_l and d_l in (6) can be computed through some algebraic manipulations, and a notable limit involving the Meijer–G function, $G_{p,q}^{m,n}\left(z\middle| \begin{smallmatrix}(a_p)\\(b_q)\end{smallmatrix}\right)$, for $z \to -1$ and $p = q$. First of all, let us multiply and divide $\mathcal{F}_l\left(\cdot\right)$ in (2) by $\left[1 - s^2/\left(s+\mathcal{X}_{1,l}\right)\left(s+\mathcal{X}_{2,l}\right)\right]^{\left(\omega_{1,l}+\omega_{2,l}-1\right)}$. Thus, (2) can be rewritten as $\mathcal{F}_l\left(s\right) = \mathcal{F}_l^{(1)}\left(s\right)\mathcal{F}_l^{(2)}\left(s\right)$ with:

$$\begin{aligned}\mathcal{F}_l^{(1)}\left(s\right) = &\left[1 - \frac{s^2}{\left(s+\mathcal{X}_{1,l}\right)\left(s+\mathcal{X}_{2,l}\right)}\right]^{\left(\omega_{1,l}+\omega_{2,l}-1\right)} \\ &\times G_{2,2}^{1,2}\left(-\frac{s^2}{\left(s+\mathcal{X}_{1,l}\right)\left(s+\mathcal{X}_{2,l}\right)}\middle| \begin{matrix}1-\omega_{2,l} & 1-\omega_{1,l}\\ 0 & 0\end{matrix}\right)\end{aligned} \tag{7}$$

$$\begin{aligned}\mathcal{F}_l^{(2)}\left(s\right) = &\mathcal{K}_l\left(s+\mathcal{X}_{1,l}\right)^{-\omega_{1,l}}\left(s+\mathcal{X}_{2,l}\right)^{-\omega_{2,l}} \\ &\times\left[1 - \frac{s^2}{\left(s+\mathcal{X}_{1,l}\right)\left(s+\mathcal{X}_{2,l}\right)}\right]^{-\left(\omega_{1,l}+\omega_{2,l}-1\right)}\end{aligned} \tag{8}$$

By studying (7) and (8) for $|s| \to \infty$, we obtain:

$$\lim_{|s|\to\infty}\left|\mathcal{F}_l^{(1)}\left(s\right)\right| = \Gamma\left(\omega_{1,l}+\omega_{2,l}-1\right) + o\left(1\right) \tag{9}$$

$$\lim_{|s|\to\infty}\left|\mathcal{F}_l^{(2)}\left(s\right)\right| = \mathcal{K}_l\left(\mathcal{X}_{1,l}+\mathcal{X}_{2,l}\right)^{-\left(\omega_{1,l}+\omega_{2,l}-1\right)}\left|s\right|^{-1} + o\left(\left|s\right|^{-1}\right) \tag{10}$$

where (9) arises from the notable limit in [14, Eq. (8.2.2.59)][1], and (10) follows after some algebraic manipulations.

By comparing (6) with (9) and (10), we get b_l in (4), $d_l = 1$, and $d = \sum_{l=1}^{L} d_l = L$. Finally, the application of [16, Prop. 3] and [16, Eq. (1)] leads to (3). This concludes the proof. □

IV. Application to SSK Modulation

As an example, let us consider the application of *Proposition 1* to the computation of ABEP, diversity gain, and coding gain of SSK modulation. Two case studies are considered: i) independent fading at both transmitter and receiver (*case study 1*); and ii) correlated fading at the transmitter and independent fading at the receiver (*case study 2*).

[1]If $|s| \to \infty$, then $z = -s^2\left(s+\mathcal{X}_{1,l}\right)^{-1}\left(s+\mathcal{X}_{2,l}\right)^{-1} \to -1$.

The ABEP of SSK modulation can be tightly upper–bounded as follows [11, Eq. (35)]:

$$\mathrm{ABEP} \le \frac{1}{N_t\log_2\left(N_t\right)}\sum_{t_1=1}^{N_t}\sum_{t_2=1}^{N_t} N_H\left(t_1,t_2\right)\mathrm{PEP}\left(t_1\to t_2\right) \tag{11}$$

where N_t are the antennas at the transmitter, $N_H\left(t_1,t_2\right)$ is the Hamming distance between the antenna–indexes t_1 and t_2, and $\mathrm{PEP}\left(t_1\to t_2\right)$ is the Pairwise Error Probability (PEP) of antenna–indexes t_1 and t_2, which is defined as:

$$\mathrm{PEP}\left(t_1\to t_2\right) = \frac{1}{\pi}\int_0^{\pi/2}\left[\prod_{r=1}^{N_r}\mathcal{M}_{t_1,t_2}^{(r)}\left(\frac{E_m}{4N_0}\frac{1}{2\sin^2\left(\theta\right)}\right)\right]d\theta \tag{12}$$

where N_r are the antennas at the receiver, and E_m/N_0 is the symbol–energy–to–noise–spectral–density ratio.

In *case study 1*, $\mathcal{M}_{t_1,t_2}^{(r)}\left(\cdot\right)$ is given in (2), where $\left(m_{t,r},\Omega_{t,r}\right)$ are the parameters of the Nakagami–*m* fading on the wireless link from the t–th transmit antenna to the r–th receive antenna, and [11, Sec. III–B]: $\mathcal{K}_l \mapsto \mathcal{K}_{t_1,t_2}^{(r)} = \left(m_{t_1,r}^{m_{t_1,r}}m_{t_2,r}^{m_{t_2,r}}\right)/\left[\Omega_{t_1,r}^{m_{t_1,r}}\Omega_{t_2,r}^{m_{t_2,r}}\Gamma\left(m_{t_1,r}\right)\Gamma\left(m_{t_2,r}\right)\right]$; $\mathcal{X}_{1,l} \mapsto \mathcal{X}_{t_1}^{(r)} = m_{t_1,r}/\Omega_{t_1,r}$; $\mathcal{X}_{2,l} \mapsto \mathcal{X}_{t_2}^{(r)} = m_{t_2,r}/\Omega_{t_2,r}$; $\omega_{1,l} \mapsto \omega_{t_1}^{(r)} = m_{t_1,r}$; and $\omega_{2,l} \mapsto \omega_{t_2}^{(r)} = m_{t_2,r}$ for $t_1,t_2 = 1,2,\ldots,N_t$ and $r = 1,2,\ldots,N_r$.

In *case study 2*, $\mathcal{M}_{t_1,t_2}^{(r)}\left(\cdot\right)$ is given by [11, Sec. III–C]:

$$\mathcal{M}_{t_1,t_2}^{(r)}\left(s\right) = \sum_{k=0}^{+\infty}\left[\frac{\mathcal{C}_{t_1,t_2,r}^{m_r+2k-1}}{2^{m_r-1}4^k\left(k!\right)\Gamma\left(k+m_r\right)}\Psi_{t_1,t_2,r}^{(k)}\left(s\right)\right] \tag{13}$$

where $\left(\cdot!\right)$ denotes factorial; $m_{t,r} = m_r$ for $t = 1,2,\ldots,N_t$; $\rho_{t_1,t_2,r}$ is the correlation coefficient between the wireless link from the t_1–th transmit antenna to the r–th receive antenna and the wireless link from the t_2–th transmit antenna to the r–th receive antenna; $\mathcal{C}_{t_1,t_2,r} = \left(2m_r\sqrt{\rho_{t_1,t_2,r}}\right)/\left[\sqrt{\Omega_{t_1,r}\Omega_{t_2,r}}\left(1-\rho_{t_1,t_2,r}\right)\right]$; and $\Psi_{t_1,t_2,r}^{(k)}\left(\cdot\right)$ is given in (2) with: $\mathcal{K}_l \mapsto \mathcal{K}_{t_1,t_2}^{(r)} = m_r^{m_r+1}\Big/\left[\Gamma\left(m_r\right)\Omega_{t_1,r}\Omega_{t_2,r}\left(1-\rho_{t_1,t_2,r}\right)\left(\sqrt{\Omega_{t_1,r}\Omega_{t_2,r}\rho_{t_1,t_2,r}}\right)^{m_r-1}\right]$; $\mathcal{X}_{1,l} \mapsto \mathcal{X}_{t_1}^{(r)} = m_r/\left[\Omega_{t_1,r}\left(1-\rho_{t_1,t_2,r}\right)\right]$; $\mathcal{X}_{2,l} \mapsto \mathcal{X}_{t_2}^{(r)} = m_r/\left[\Omega_{t_2,r}\left(1-\rho_{t_1,t_2,r}\right)\right]$; $\omega_{1,l} \mapsto \omega_{t_1}^{(r)} = m_r + k$; and $\omega_{2,l} \mapsto \omega_{t_2}^{(r)} = m_r + k$.

Accordingly, from *Proposition 1*, the PEP in (12) can be written as shown in (14) and (15) on top of the next page for *case study 1* and *case study 2*, respectively. As far as *case study 2* is concerned, b_{k_r} for $r = 1,2,\ldots,N_r$ are defined in (4) with the fading parameters summarized in (13). From (14) and (15), coding and diversity gains can be obtained in closed–form from [16, Eq. (1)]. In particular, the diversity gain is $G_d = N_r$, which is independent of the fading severity $m_{t,r}$. This result is substantially different with respect to conventional modulation schemes, where, for Nakagami–*m* fading, G_d depends on both $m_{t,r}$ and N_r [15, Sec. 9.6.4].

V. Framework Validation

In this section, we study the accuracy of *Proposition 1*, and, in particular, the tightness of (14) and (15) for SSK modulation. Without loss of generality, we consider an identically distributed (and correlated) fading scenario in which the fading parameters are all the same, *i.e.*, $\left(m_{t.r},\Omega_{t,r},\rho_{t_1,t_2,r}\right) =$

$$\mathrm{PEP}\left(t_1 \to t_2\right) = \frac{2^{N_r-1}\left[\prod\limits_{r=1}^{N_r} \frac{m_{t_1,r}^{m_{t_1,r}} m_{t_2,r}^{m_{t_2,r}}}{\Omega_{t_1,r}^{m_{t_1,r}} \Omega_{t_2,r}^{m_{t_2,r}} \Gamma\left(m_{t_1,r}\right)\Gamma\left(m_{t_2,r}\right)} \left(\frac{m_{t_1,r}}{\Omega_{t_1,r}} + \frac{m_{t_2,r}}{\Omega_{t_2,r}}\right)^{-\left(m_{t_1,r}+m_{t_2,r}-1\right)} \Gamma\left(m_{t_1,r}+m_{t_2,r}-1\right)\right]\Gamma\left(N_r+1/2\right)}{\sqrt{\pi}\Gamma\left(N_r+1\right)} \left(\frac{E_m}{4N_0}\right)^{-N_r} \tag{14}$$

$$\mathrm{PEP}\left(t_1 \to t_2\right) = \frac{2^{N_r-1}\left[\left(\sum\limits_{k_1=0}^{+\infty} \frac{C_{t_1,t_2,r}^{m_r+2k_1-1} b_{k_1}}{2^{m_r-1}4^{k_1}(k_1!)\Gamma(k_1+m_r)}\right)\cdot\ldots\cdot\left(\sum\limits_{k_{N_r}=0}^{+\infty} \frac{C_{t_1,t_2,r}^{m_r+2k_{N_r}-1} b_{k_{N_r}}}{2^{m_r-1}4^{k_{N_r}}\left(k_{N_r}!\right)\Gamma\left(k_{N_r}+m_r\right)}\right)\right]\Gamma\left(N_r+1/2\right)}{\sqrt{\pi}\Gamma\left(N_r+1\right)} \left(\frac{E_m}{4N_0}\right)^{-N_r} \tag{15}$$

(m_0, Ω_0, ρ_0) for $t, t_1, t_2 = 1, 2, \ldots, N_t$ and $r = 1, 2, \ldots, N_r$. In this case, the ABEP in (11) simplifies as $\mathrm{ABEP} \le (N_t/2)\,\mathrm{PEP}\left(t_1 \to t_2\right) = (N_t/2)\,\mathrm{PEP}_0$, where $\mathrm{PEP}_0 = \mathrm{PEP}\left(t_1 \to t_2\right)$ is given in (14) and (15), and it is the same for any pair (t_1, t_2). Also, we have used the identity $\sum_{t_1=1}^{N_t}\sum_{t_2=1}^{N_t} N_H\left(t_1, t_2\right) = \left(N_t^2/2\right)\log_2\left(N_t\right)$. The comparison among Monte Carlo simulations, the numerical integration of (1), and the high SNR framework in (14) and (15) is shown in Fig. 1. The curves confirm the tightness of our framework and the correctness of our analytical derivation.

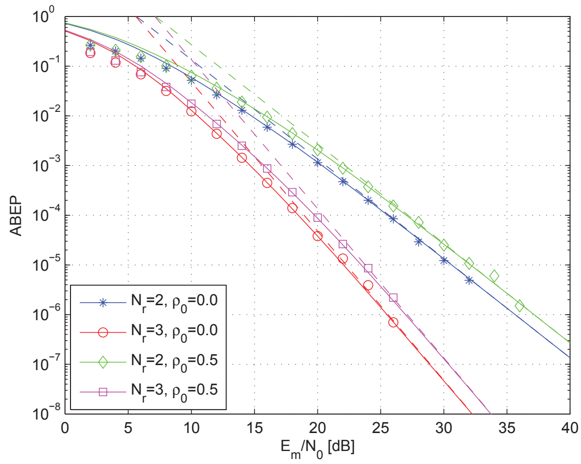

Fig. 1. Setup: $N_t = 8$, $\Omega_0 = 1$, and $m_0 = 2.5$. Markers: Monte Carlo simulation. Solid lines: numerical integration in (1). Dashed lines: high SNR framework in (14) and (15).

VI. Concluding Remarks

In this Letter, we have introduced a new framework to compute the ABEP of space modulation over correlated Nakagami–*m* fading. The framework enables a simple computation of coding and diversity gains. We have proved that the diversity gain of SSK modulation is independent of the fading severity. By using [10], the framework is applicable to generic SM–MIMO as well. In particular, from [10] we know that the ABEP of SM is the linear combination of the ABEP of conventional PSK/QAM and SSK modulation. Thus, from *Proposition 1* we conclude that the diversity gain of SM is the minimum between the diversity gains of PSK/QAM and SSK modulation. Finally, we note that if space modulation is enhanced with transmit–diversity capabilities [7]–[9], [13], coding and diversity gains can be computed by using standard analytical frameworks, *e.g.*, [15], [16]. This follows directly from [13, Eq. (24)]. Furthermore, in this case the fading severity *m* will affect the diversity gain as in conventional PSK/QAM modulation.

Acknowledgment

We gratefully acknowledge support from the European Union (PITN–GA–2010–264759, GREENET project) for this work. M. Di Renzo acknowledges support of the Laboratory of Signals and Systems (L2S) under the research project “Jeunes Chercheurs”. H. Haas acknowledges the EPSRC (EP/G011788/1) and the Scottish Funding Council support of his position within the Edinburgh Research Partnership in Engineering and Mathematics.

References

[1] Y. Chau and S.–H. Yu, “Space modulation on wireless fading channels”, *IEEE Veh. Technol. Conf. – Fall*, vol. 3, pp. 1668–1671, Oct. 2001.

[2] Y. Yang and B. Jiao, “Information–guided channel–hopping for high data rate wireless communication”, *IEEE Commun. Lett.*, vol. 12, pp. 225–227, Apr. 2008.

[3] R. Y. Mesleh *et al.*, “Spatial modulation”, *IEEE Trans. Veh. Technol.*, vol. 57, pp. 2228–2241, July 2008.

[4] J. Jeganathan *et al.*, “Space shift keying modulation for MIMO channels”, *IEEE Trans. Wireless Commun.*, vol. 8, pp. 3692–3703, July 2009.

[5] M. Di Renzo and H. Haas, “Improving the performance of space shift keying (SSK) modulation via opportunistic power allocation”, *IEEE Commun. Lett.*, vol. 14, pp. 500–502, June 2010.

[6] R. Y. Mesleh *et al.*, “Trellis coded spatial modulation”, *IEEE Trans. Wireless Commun.*, vol. 9, pp. 2349–2361, July 2010.

[7] S. Sugiura, S. Chen, and L. Hanzo, “Coherent and differential space–time shift keying: A dispersion matrix approach”, *IEEE Trans. Commun.*, vol. 11, pp. 3219–3230, Nov. 2010.

[8] E. Basar *et al.*, “Space–time block coded spatial modulation”, *IEEE Trans. Commun.*, vol. 59, pp. 823–832, Mar. 2011.

[9] S. Sugiura, S. Chen, L. Hanzo, “Generalized space–time shift keying designed for flexible diversity–, multiplexing– and complexity–tradeoffs”, *IEEE Trans. Wireless Commun.*, vol. 11, pp. 1144–1153, Apr. 2011.

[10] M. Di Renzo and H. Haas, “Performance analysis of spatial modulation”, *IEEE Int. Conf. Commun. Netw. in China*, pp. 1–7, Aug. 2010.

[11] —, “A general framework for performance analysis of space shift keying (SSK) modulation for MISO correlated Nakagami–*m* fading channels”, *IEEE Trans. Commun.*, vol. 58, pp. 2590–2603, Sep. 2010.

[12] —, “Space shift keying (SSK) modulation with partial channel state information: Optimal detector and performance analysis over fading channels”, *IEEE Trans. Commun.*, vol. 58, pp. 3196–3210, Nov. 2010.

[13] —, “Space shift keying (SSK–) MIMO over correlated Rician fading channels: Performance analysis and a new method for transmit–diversity”, *IEEE Trans. Commun.*, vol. 59, pp. 116–129, Jan. 2011.

[14] A. P. Prudnikov, Y. A. Brychkov, and O. I. Marichev, *Integrals and Series. Vol. 3: More Special Functions*, 2003.

[15] M. K. Simon and M.–S. Alouini, *Digital Communication over Fading Channels*, John Wiley & Sons, Inc., 1st ed., 2000.

[16] Z. Wang and G. B. Giannakis, “A simple and general parameterization quantifying performance in fading channels”, *IEEE Trans. Commun.*, vol. 51, pp. 1389–1398, Aug. 2003.